

## Kinematic and Kinetic Analysis of the Lumbar and Pelvis of Highly Reclined Occupants Under Varied Rigid Seat Configurations Using a Human Body Model

Qiang Wang, Yu Liu, XiaoTing Yang, JieMing Li, Jing Fei, ZhongHao Bai

**Abstract** The diverse postures of occupants in intelligent vehicles present new challenges to collision safety. This study aims to investigate the kinematic and kinetic responses of the lumbar spine and pelvis under various reclined seat configurations. Using a validated adjustable rigid seat system, 13 seat configurations with varying seatback and seatpan angles were designed, incorporating four levels of seat opening angles. Based on cadaveric test pulses, THUMS Version 7 was employed to analyse the motion and loading of the lumbar spine and pelvis during frontal impacts in reclined postures. The results indicate that increasing the seatback angle leads to significant hip sliding and posterior rotation of the lumbar spine and pelvis. The effect of seatback angle variation on the peak axial compression force of the lumbar spine differs under various seatpan angle levels. Highly reclined seatback angles and larger seat opening angles result in significant lumbar extension moments. These findings contribute to the optimisation of occupant protection design for reclined seat configurations.

**Keywords** Reclined posture, lumbar spine, pelvis, Human Body Model, rigid seat.

### I. INTRODUCTION

With the rise of intelligent vehicles, the interior layouts have become increasingly diverse, enabling more flexible occupant postures, including reclined positions, to enhance comfort. Adjustable seatback and seatpan angles are now available for both front and rear seats, significantly improving the riding experience [1-2]. However, these diverse configurations raise critical safety concerns in collision scenarios.

Studies have shown that varying seatback angles cause significant differences in lumbar spine alignment and pelvic orientation [3-4]. The pelvis and lumbar spine exhibit distinct motion responses and load transfer mechanisms in reclined postures compared to upright ones. Low-severity volunteer tests reveal that greater torso inclination leads to more pronounced hip displacement [5-6], while post-mortem human subject (PMHS) tests in reclined postures show a higher likelihood of iliac and lumbar spine fractures during high-speed frontal collisions [7-9]. These findings underscore the importance of pelvic and lumbar responses in occupant injuries associated with reclined postures. Existing research focuses primarily on torso angle variations caused by seatback adjustments, often keeping cushion angles constant. However, cushion angles also significantly affect pelvic motion. An elevated seat cushion can restrict pelvic movement but may increase lumbar spine loading [10]. Despite these interactions, limited research systematically investigates the combined effects of seatback and cushion angle variations on pelvic and lumbar responses.

Volunteer and PMHS tests are constrained by ethical restrictions, and Anthropomorphic Test Devices (ATDs) like THOR 50M and Hybrid-III 50M are unsuitable for large torso angles due to their mechanical limitations [11]. Newly developed dummies, such as THOR-AV and THOR-RS, have shown potential in reclined postures [12-13] but remain insufficiently validated. Human Body Models (HBMs) provided an effective alternative, closely replicating anatomical structures and capturing detailed kinematic, kinetic, and biomechanical data [14-15]. THUMS (Total Human Model for Safety) Version 7 has been validated against PMHS experiments and includes models with torso angles of 25°, 35° and 45° [16]. These postures are adjusted based on X-ray data, capturing spine morphology in reclined positions. However, the degree of recline is limited and further validation of torso and neck angles is needed. Thus, studying the kinematic and kinetic responses of the pelvis and lumbar spine under various seatback and seatpan configurations using HBMs in diverse reclined postures is crucial. This research will help to clarify the mechanisms behind increased injury risk in highly reclined positions.

## II. METHODS

### Simulation Environment

The simulation setup features a rigid seat with independently adjustable angles for the seatback, seatpan, and leg support (Fig. 1). The seatbelt, supplied by Autoliv, includes a shoulder-belt load limiter but lacks a pretensioner or other restraint components. The D-ring is integrated into the upper right side of the seatback, while the anchor point is fixed to the right side. The buckle rotates around a fixed axis. This system has been used in previous high-speed frontal sled tests with the THOR-AV dummy and validated finite element (FE) models [15]. The input pulse was based on high-speed PMHS tests, with a 50 km/h velocity change and a 34 g peak acceleration [7] (Fig. 1).



Fig. 1. Rigid seat angles setup (left); pulse from [7] (right).

### HBM Positioning

Thirteen seat configurations were designed using the adjustable rigid seat, including four seatpan angles and four seat opening angles. The leg support was fixed relative to the seatpan (Appendix, Table A1). The baseline configuration was defined as a 15° seatpan angle and a 25° seatback angle. THUMS V7 models for three reclined postures were adjusted using regression equations predicting pelvic, lumbar, thoracic, neck, and head angles [3]. Posture adjustments were performed in PRIMER software (Version 17.1, Oasys Ltd), starting with pelvic rotation to align with the predicted orientation, followed by sequential rotations of the lumbar, thoracic, and cervical spine around joint centres. Leg angles were adjusted to fit with the seatpan and leg support, and arms rested naturally on the thighs. Four baseline models were created: BA-CA configurations 25-15, 35-15, 45-15, and 55-15, with the latter two derived from the 45° THUMS V7 model (Appendix, Fig. A1).

The baseline configuration's reference H-point was measured using the H-point machine (HPM) in physical tests. H-point coordinates for the four baseline models were calculated based on [3]'s regression function between the H-point and seatback angle. Adjusted H-point, torso, and spinal angles are shown in Table A11 in the Appendix. Since the regression function did not account for seatpan angle variation, the study assumed that at large seatback angles, the body rotates with the seat while maintaining its relative position. By rotating baseline models about the seat axis, additional configurations with consistent seat opening angle were generated. Identical nodes defined the seatbelt path across all models to ensure alignment of the shoulder belt with the midpoint of the right clavicle and sternum, while the lap belt conformed to the groin. The buckle was rotated to align with the iliac wing, and anchor points were fixed.

### Data Processing

The study examined lumbar spine and pelvic kinematic and kinetic responses. Kinematic responses included head and pelvic displacements, lumbar spine and pelvic rotations, with the X-axis positive forward, Z-axis upward, and Y-axis rotation positive in forward flexion. Kinetic responses included Z-axis compressive forces, Y-axis flexion moments in the lumbar vertebrae, and ASIS (anterior superior iliac spine) forces at the pelvis. Compressive forces and flexion moments were considered positive. Lap-belt and seatpan contact forces were measured, and animations reviewed to confirm proper seatbelt alignment with the iliac crest to prevent submarining. The simulation duration was 160 ms.

## III. RESULTS

### Kinematic Response

All 13 simulation cases were completed without any evidence of submarining. Figure 2 shows the maximum head

and hip displacements. At the same seatpan angle, increasing the seatback angle slightly reduced the maximum X-direction displacement of the head. A higher seatpan angle also marginally decreased the head's X-direction displacement. Conversely, at the same seatpan angle the hip's maximum X-direction displacement significantly increased with a larger seatback angle, while a higher seatpan angle slightly reduced it. For smaller seatpan angles, increasing the seatback angle notably reduced the head's maximum Z-direction displacement. However, as the seatpan angle rose, the head's Z-direction displacement gradually increased. Similarly, the hip's maximum Z-direction displacement progressively increased for the same seatpan angle.

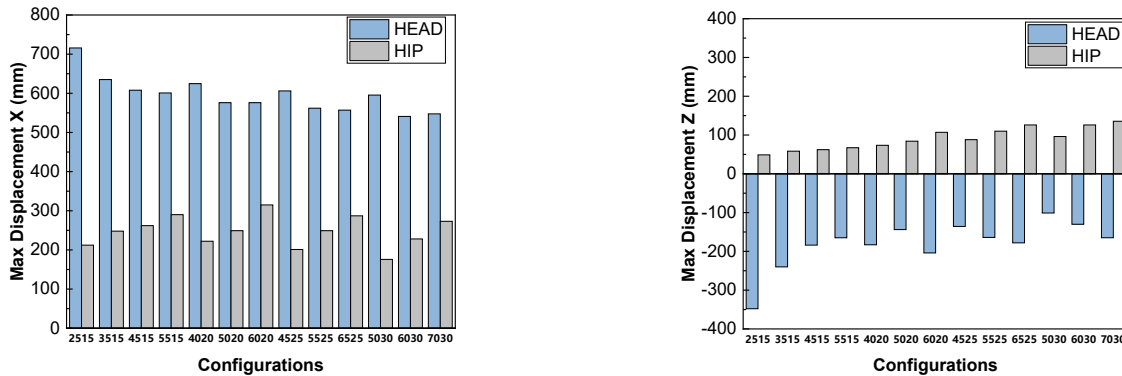


Fig. 2. Maximum displacement of head and HIP in X (left) and Z (right) direction.

The rotational behaviour of the lumbar spine (L1) and pelvis was analysed using L1 and HIP markers (Fig. 3). In the baseline posture, L1 showed significant anterior rotation. At a seatpan angle from 15° to 25°, increasing the seatback angle gradually reduced anterior rotation, eventually causing posterior rotation. At a seatpan angle of 30°, a larger seatback angle amplified L1 posterior rotation. The pelvis followed a similar trend: increasing the seatback angle reduced anterior rotation and led to posterior rotation. Greater seat opening angles increased the likelihood of posterior rotation in both L1 and the pelvis.

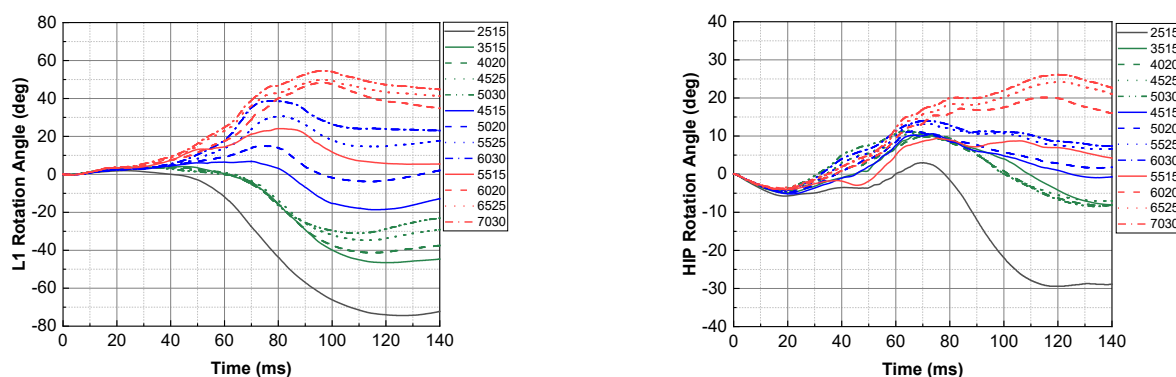


Fig. 3. Local rotation of L1 (left) and pelvis (right).

### Kinetic Response

Compared to an upright posture, peak lumbar forces increased across all non-standard postures (Fig. 4). At a seatpan angle of 15°, the peak lumbar compressive force initially rose and then declined as the seatback angle increased. For seatpan angles of 20°–30°, the peak axial compressive force progressively decreased with increasing seatback angle. Overall, greater seat opening angles resulted in lower peak lumbar axial compressive forces.

The variation in peak lumbar flexion and extension moments (L3–L5) along the Y-axis was analysed (Appendix, Fig. A2). At the same seatpan angle, increasing the seatback angle notably reduced peak lumbar flexion moments. Extension moments became significant when the seatback angle exceeded 55°, and a seat opening angle of 130° produced high peak extension moments across the L3–L5 segments.

Figure 4 shows peak forces on the iliac crest, lap belt, and seatpan. At the same seatpan angle, increasing the seatback angle led to higher ASIS and lap-belt forces. For a 15° seatpan angle, seatpan force initially increased and then decreased with seatback angle changes. For larger seatpan angles (25°–30°), seatpan force decreased significantly as the seatback angle increased.

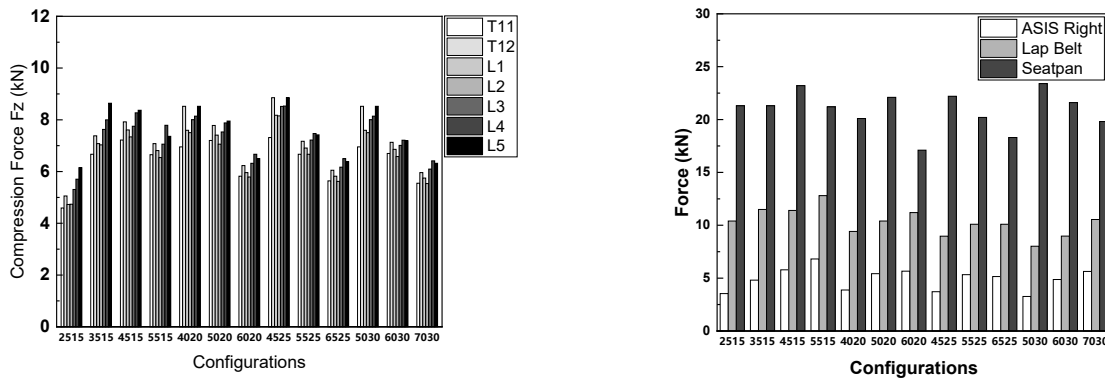


Fig. 4. Compression force Fz in T11-L5 (left); ASIS Right force, lap-belt force and seatpan contact force (right).

#### IV. DISCUSSION

In all simulations, engagement between the lap belt and the iliac crest was consistently maintained. Even under seat configurations where the seatback angle exceeded 60°, no instances of lap belt submarining into the abdominal region were observed. This can be attributed to two factors. First, the rigid seat design prevented deformation of the seatpan, common in production seats, thereby reducing downward pelvic movement. Second, the study paired larger seatback angles with greater seatpan angles, with the elevated seatpan angle effectively resisting submarining.

Increased seatback angles led to greater pelvic displacement, aligning with previous research [5][15]. At larger angles, the pelvis began in a more rearward position with greater posterior tilt, which altered lap-belt alignment with the iliac crest and reduced restraint effectiveness. Additionally, as seatback angles increased, the pelvis transitioned from anterior to pronounced posterior rotation during forward motion. This may be due to the centre of gravity of the upper torso lowering and shifting rear, consistent with PMHS experiment observations [7]. A higher seatpan angle amplified this posterior rotation by moving the hips' centre of gravity upward relative to the upper torso during forward motion.

The lumbar spine at the L1 segment exhibited greater variability compared to the pelvis but followed a similar trend. In upright postures, the upper lumbar spine showed anterior rotation, while at seatback angles exceeding 60° it demonstrated pronounced posterior rotation. The lumbar spinal load also varied with changes in recline angle. At smaller seatpan angles, increasing recline led to higher lumbar compressive forces. However, at larger seatpan angles, compressive forces decreased with increasing recline. Notably, the configuration with the largest seat open angle significantly reduced lumbar compressive forces in all reclined postures. This suggests that an optimised combination of recline and seatpan angles could improve lumbar loading in highly reclined postures. The lumbar spine also experienced extension moments at larger recline angles, consistent with earlier findings [8][15]. Larger seat open angles were associated with increased extension moments, likely due to changes in lumbar rotational movement. These results indicate that in highly reclined postures during collisions, the lumbar spine may experience a combined extension and compression loading pattern, in addition to the commonly observed flexion and compression loads [17].

This study has limitations. The simulations employed a simplified rigid seat, which lacks the characteristics of real-world seats, necessitating further evaluation. Additionally, only a basic three-point seatbelt with a force limiter was used, without advanced restraint components like anchor and buckle pretensioners, crash locking tongue, or supplementary in-vehicle structures. Future research should validate these findings in more realistic vehicle environments. Furthermore, this study utilised only the THUMS model to analyse pelvis and lumbar spine kinematics and kinetics. Future work should incorporate a variety of HBMs and extend the analysis to whole-body kinematics and biomechanical responses across critical regions.

#### V. CONCLUSION

This study used a simplified, validated rigid seat system to design 13 seat configurations with varying seatback and seatpan angles. Using the THUMS V7 model, it analysed lumbar spine and pelvis motion and loading in reclined postures during frontal collisions. Results showed that increased seatback angles caused significant hip slippage and posterior rotation of the lumbar spine and pelvis. Peak lumbar spine axial compressive forces varied with seatback and seatpan angle changes. Highly reclined seatback angles and larger seat opening angles led to

significant lumbar spine extension moments. These findings aid occupant protection design for high-recline seating configurations.

## VI. REFERENCES

- [1] Jorlöv, S., Bohman, K. & Larsson, A. (2017) Seating positions and activities in highly automated cars—a qualitative study of future automated driving scenarios. *Proceedings of the IRCOBI Conference, 2017*, Antwerp, Belgium, pp. 13–22.
- [2] Östling, M. & Larsson, A. (2019) Occupant activities and sitting positions in automated vehicles in China and Sweden. *Proceedings of the 26th International Technical Conference on the Enhanced Safety of Vehicles (ESV)*, 2019, Eindhoven, Netherlands, pp. 10–13.
- [3] Reed, M. P., Ebert, S. M. & Jones, M. L. (2019) Posture and belt fit in reclined passenger seats. *Traffic Injury Prevention*, **20**(sup1): pp. S38–S42.
- [4] Izumiyama, T., Nishida, N., *et al.* (2022) Analysis of individual variabilities for lumbar and pelvic alignment in highly reclined seating postures and occupant kinematics in a collision. *Proceedings of the IRCOBI Conference, 2022*, Porto, Portugal, pp. 941–955.
- [5] Muehlbauer, J., Schick, S., *et al.* (2019) Feasibility study of a safe sled environment for reclined frontal deceleration tests with human volunteers. *Traffic Injury Prevention*, **20**(sup2): pp. S171–S174.
- [6] González-García, M., Siebler, L., *et al.* (2023) Kinematic response of seated male volunteers in various reclined postures on a sled subjected to a braking pulse. *Accident Analysis and Prevention*, **193**: 107293.
- [7] Richardson, R., Donlon, J. P., *et al.* (2021) Kinematic and injury response of reclined PMHS in frontal impacts. SAE Technical Paper, No. 2020-22-0004.
- [8] Baudrit, P., Uriot, J., Richard, O. & Debray, M. (2023) Investigation of potential injury patterns and occupant kinematics in frontal impact with PMHS in reclined postures. *Stapp Car Crash Journal*, 66.
- [9] UMTRI (2021) University of Michigan Transportation Research Institute. Automated Vehicle Occupant Kinematics. NHTSA Test Report.
- [10] Tang, L., Zheng, J., Zhou, Q. (2020) Investigation of risk factors affecting injuries in reclining seat under frontal impact. *International Journal of Vehicle Safety*, **11**(3): pp. 247–74.
- [11] Shin, J., Donlon, J. P., *et al.* (2022) Biofidelity evaluation of the Hybrid-III 50th male and THOR-50M in reclined frontal impact sled tests. *Proceedings of the IRCOBI Conference, 2022*, Porto, Portugal, pp. 309–331.
- [12] Wang, Z. J., Zaseck, L. W., Reed, M. P. (2022) THOR-AV 50th percentile male biofidelity evaluation in 25° and 45° seatback angle test conditions with a semi-rigid seat. *Proceedings of the IRCOBI Conference, 2022*, Porto, Portugal, pp. 401–417.
- [13] Lozano, P., Roka, S., *et al.* (2023) Comparison of the Injury Risk Prediction of the THOR-Reclined Dummy and the THUMS HBM. *Proceedings of the 27th International Technical Conference on the Enhanced Safety of Vehicles (ESV)*, 2023, Yokohama, Japan, No. 23-0302.
- [14] Gepner, B. D., Perez-Rapela, D., *et al.* (2022) Evaluation of GHBM, THUMS and SAFER human body models in frontal impacts in reclined postures. *Proceedings of the IRCOBI Conference, 2022*, Porto, Portugal, pp. 116–143.
- [15] Fei, J., Liu, Y., *et al.* (2024) Comparison of Responses Between Human Body Model and Anthropomorphic Test Device Model in Reclined Postures. *Proceedings of the IRCOBI Conference, 2024*, Stockholm, Sweden, pp. 25, 30.
- [16] Matsuda, T., Kobayashi, N., Fujita, N. & Kitagawa, Y. (2023) Development of a human body model (THUMS Version 7) to simulate kinematics and injuries of reclined occupants in frontal collisions. *Proceedings of the 27th Enhanced Safety of Vehicles (ESV) Conference*, 2023, Yokohama, Japan.
- [17] Tushak, S. K., Donlon, J. P., *et al.* (2022) Failure tolerance of the human lumbar spine in kinetic combined compression and flexion loading. *Journal of Biomechanics*, **135**: 111051.

## VII. APPENDIX

TABLE AI  
SEAT CONFIGURATIONS

Conditions	Seatpan Angle/deg.	Seatback Angle/deg.	Seat Opening Angle/deg.
2515(Baseline)	15	25	100
3515	15	35	
4020	20	40	110
4525	25	45	
5030	30	50	
4515	15	45	
5020	20	50	120
5525	25	55	
6030	30	60	
5515	15	55	
6020	20	60	130
6525	25	65	
7030	30	70	

TABLE AII  
POSTURE PARAMETERS OF TORSO AND SPINE

Posture parameters	25° Model	35° Model	45° Model	55° Model
<i>Pelvis Angle (deg.)</i>	56.3	61.6	64.9	68.2
<i>Lumbar Angle (deg.)</i>	22.3	28.5	38.7	48.8
<i>Thorax Angle (deg.)</i>	10.5	19.6	28.8	38.0
<i>Neck Angle (deg.)</i>	1.2	17.2	23.0	28.9
<i>Lumbar lordosis (deg.)</i>	9.8	6.4	16.96	18.2
<i>Thoracic kyphosis (deg.)</i>	19.4	24.6	20.7	22.7

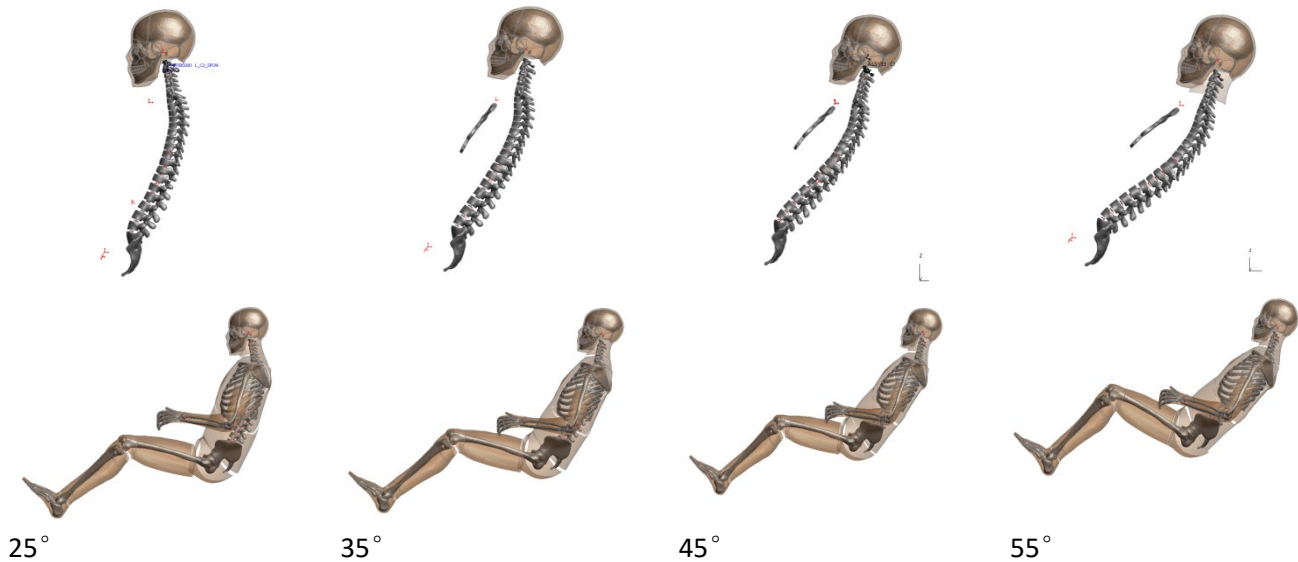


Fig. A1. Whole-body postures and spine shape of four reclined THUMS models.

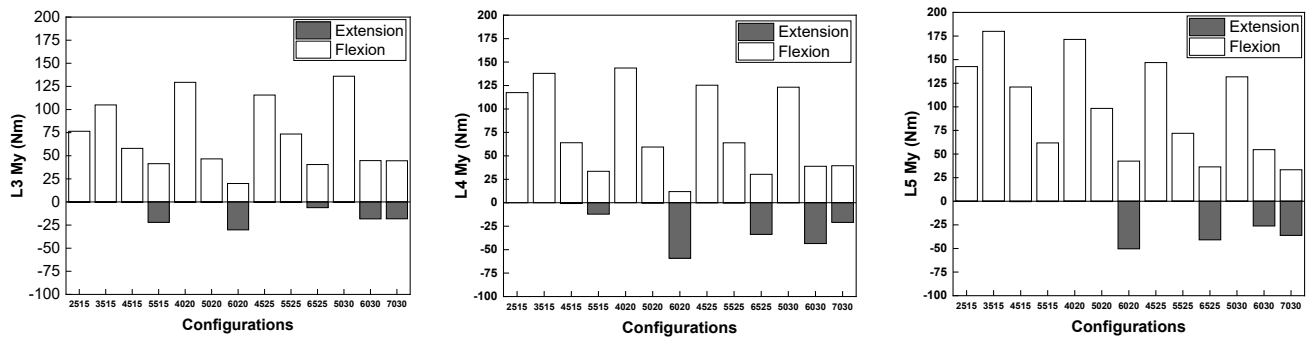


Fig. A2. Moment in Y direction of L3-L5.